A Temperature Responsive Copper Molybdate Polymorph Mixture Near to Water Boiling Point by a Simple Cryogenic Quenching Route

Nina Joseph*, Jobin Varghese, Merja Teirikangas, and Heli Jantunen

Microelectronics Research Unit, Faculty of Information Technology and Electrical Engineering, University of Oulu, Finland, P.O. Box 4500, FI-90014.

*Corresponding author: Nina Joseph

Email: ninajoseph11@gmail.com

Abstract

Smart temperature responsive inorganic materials in accessible temperature ranges open up new positions in the technology. Herein, we present for the first time a $CuMoO_4$ polymorph mixture preparedby a simple cryogenic quenching approach, which offers a fast temperature response close towater boiling temperaturefor use asa permanent temperature recorder. The new cryogenic quenching technique initiates the formation of a unique polymorph mixture of a deep brown color with a non-uniform combination of γ and α-$CuMoO_4$, with the γ phase confined to the outer region of α-$CuMoO_4$, which has been prepared by conventional solid-state synthesis. *Insitu* structural analysis and refinement results confirmthe presence of $CuMoO_4$ α and γ polymorphs, in which the amount of γ polymorph decreases and that of the α phase increases with temperature, accounting for the irreversible thermochromic behavior. The thermal analysis reveals that the polymorph mixture exhibits a fast response with the color changing from deep brown to bright green with intermediate colors of light brown, yellowish green and light green depending on the exposure temperature as observed from reflectance measurements.

Keywords: polymorph, ceramic, thermochromism, cryogenic quenching, $CuMoO_4$

Introduction

Advanced materials are essential in the technological leaps that influence society, and hence new material innovations with unique properties such as smart materials can lead to the technological revolution of a dynamically modified environment.[1,2] A piece of ceramic, metal or polymer is generally considered passive or static, while smart materials exhibit "smartness" by their ability to detect and respond to stimuli,[3] but they are not considered intelligent due to their inability to perform advanced functions. The resulting responsive materials are already exerting their influence on the existing environment as the building blocks for developing functional and smart complex systems in the form of sensors, smart clothing, robots, automobileand electronic parts, medical devices, packaging in the aerospace, military, biomedical, robotics, electronics, consumer industries [3-9] and they also influence the development, design and architecture of new technology.[2,3]
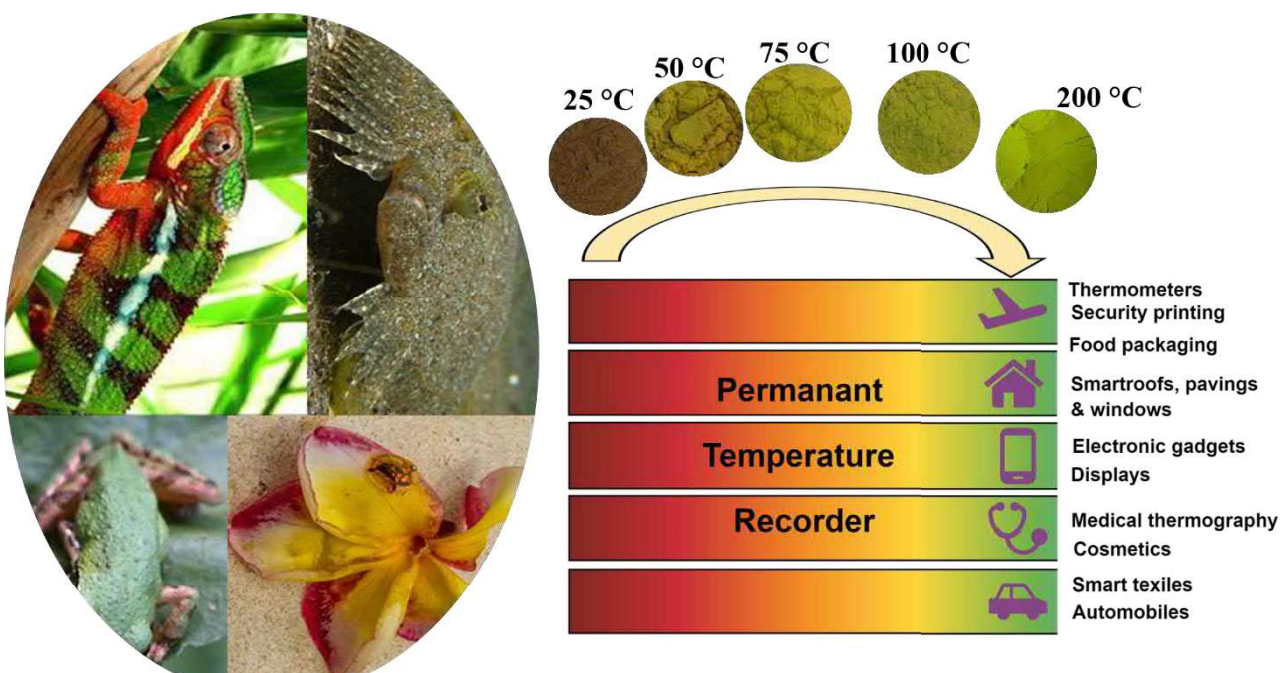
Figure 1. Chromism found in (a) nature [10] (b) inorganic $CuMoO_4$ polymorph mixture (present work) with environmental changes.

Nature is the source of smartness with a variety of living organisms. Thermochromic materials show response to environmental change by changing color. Such color changes occur naturally in the chameleon, golden tortoise beetle as shown in figure 1.[10] These materials can sense changes in the

temperaturein a manner similar to that of living beings such as animals and humans.[11] This behavior may result from a reduction of bandgap energies and ligand field on a chromophore cation,[12,13] insulating-metallic behavior transitions[14] and changes in the electronic transition energies corresponding to the extension or compression of the crystal cell, i.e. phase transition[15], which in turn affect the absorption spectrum of the material.Inorganic thermochromic materials have the advantage of better stability and longer lifetime as well as easy and cost-effective preparation over their commonly used organic counterparts.[15-32]
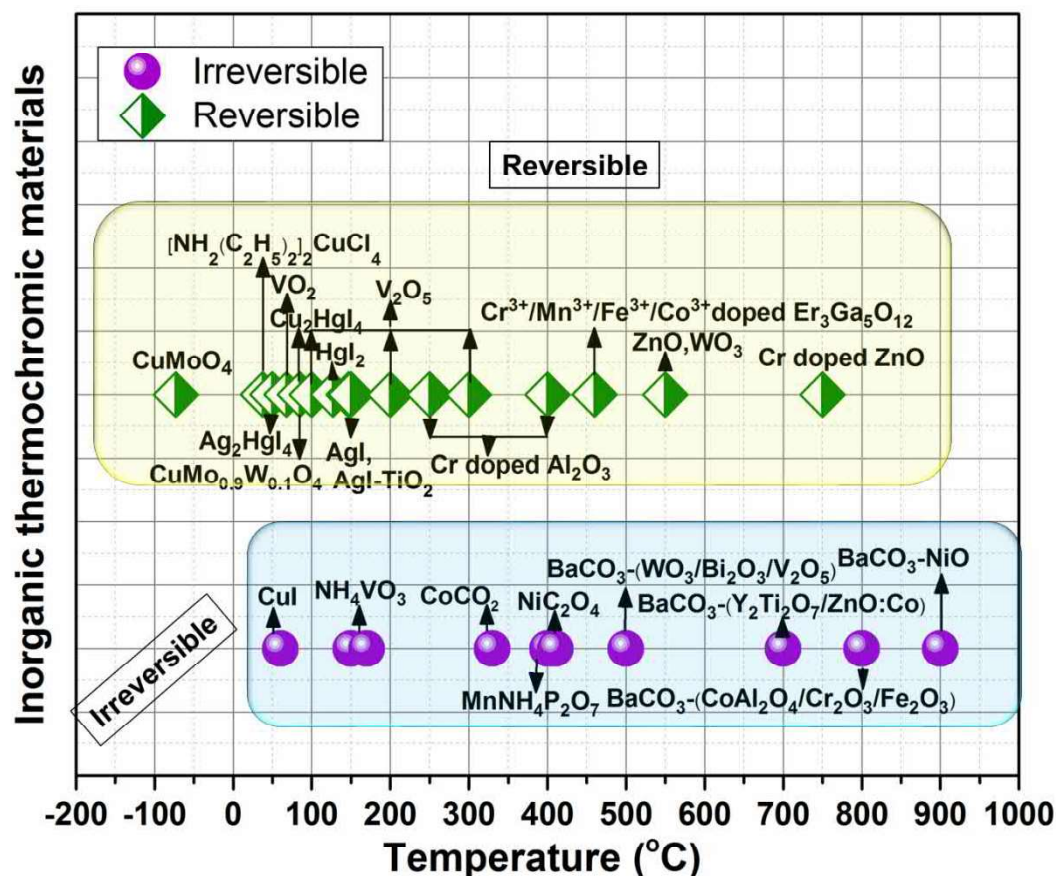
Figure 2. *Some of the reported reversible and irreversible thermochromic materials and present work*

Most of the available inorganic thermochromic metal oxides are reversible (figure 2 and table S1) and cannot be used to continuously and reliably monitor the temperature change over a period because their color changes back to its original color on cooling.[16,17,25] In contrast, irreversible materials are

one additional step towards intelligence, as their color changes cannot be reversed on cooling and provide a permanent record, which can be observed offline.[25] These materials are in high demand and are applicable as temperature-time indicators for the post analysis of some surgical operations and to monitor the storage and transportation condition of temperature-sensitive products, such as chilled and frozen foods, drugs, temperature sensitive chemicals or biological materials. They are also applicable in surface temperature distribution with a high spatial resolution, household appliances, automobile parts, hotplates, and furnaces, aeronautical engine components, electronic gadgets.[16,33,37] They form an inexpensive track and trace system that can continuously monitor the temperature as well as trace the temperature change even after the temperature stimulus has been removed. However, inorganic irreversible thermochromic dyes exhibit a high transition temperature (figure 2 & table S1) and this limits their practical use, which enhances the need for and importance of low transition temperature inorganic thermochromic materials.[15-32]

Ehrenberg et al., in 1997 reported the presence of a new γ phase in $CuMoO_4$, which is stable below -73 °C.[19] In 1997, Wiesmann et al., reported phase transition from the stable α to the γ phase in single crystal $CuMoO_4$ at atmospheric pressure by cooling at -83 °C or at room temperature by applying pressure (0.2 GPa).[38] Hernández et al., in 1999; Rodríguez et al., 2000 and Steiner et al., in 2001 revealed that $CuMoO_4$ exhibits optical contrast at the phase transition indicating its thermochromic and piezochromic behavior.[39-41] This phase transition, which results in two polymorphs, a low temperature γ (reddish brown) and a high temperature α (green) phase, corresponds to the structural rearrangement due to the first order pseudo-reconstructive phase transition.[15,19] The critical point in the color change depends on the concentration of the two phases. However, the thermochromism exhibited by this material is not in the easily accessible range as it occurs in the temperature region between ~-98 and ~-13 °C, which limits its usage for many practical applications and efforts are made to make the transition in a more useful range.[19,38] Gaudon et al., in 2007 reported tungsten-doped derivatives of $CuMoO_4$ in which $CuMo_{0.9}W_{0.1}O_4$ changes its color from red to greenby

warming above ~87 °C and from green to red by coolingbelow ~2 °C and also by applying weak pressure.[15,19,23] However, the obtained compound exhibits a reversibility in the color on cooling as well as by applying the pressure and requires a precise preparation technique to carefully optimize the composition. There are no reports, to the best of our knowledge, on the thermochromic behavior of $CuMoO_4$ in the accessible temperature range, as it is difficult to obtain the reddish brown γ phase stable at room temperatureexceptby applying pressure to α-$CuMoO_4$.[38]

In this report, the thermochromism of the $CuMoO_4$ (CMO) is tuned to around 25-200 °C (as shown in figure 1) by adjusting the concentrations of the two phases in a polymorph mixtureby simple cryogenic quenching, which in turn can open up new applications for this system. The cryogenic quenching process helps to speed up the phase transition and stabilize the formed γ phase at room temperature as the amount of both phases depends largely on the cooling rate.[18] In addition to this, the obtained mixture shows a series of color changes over the temperature range of 25-200°C (figure 1) as analyzed by the UV-Vis reflectance spectra, which makes it a suitable permanent time-temperature indicator over this temperature rangebecause it cannot be reversed by cooling. A temperature variable XRD analysis of the obtained nominal polymorph mixture gives more information on the crystal structure and composition of the compound. Figure 2 and table S1 in the supporting information giveinformation on the reported inorganic thermochromic materials, which highlights the importance and novelty of the present work.

Materials and Methods

Preparation of CuMoO₄polymorph mixture

The α-$CuMoO_4$ ceramic (CMO) was prepared by the solid-state ceramic route from the respective oxides of high purity CuO (> 99%, Alfa Aesar) and MoO_3 (> 99%, Alfa Aesar). The high purity oxides were mixed in an ethanol medium for 12 h and the mixture is then dried followed by calcination at 550 °C/12 h and sintering at 650 °C/4h, as has been reported in our previous works.[42,43]

The nominal CMO polymorph mixture was prepared by cryogenic quenching of crystalline $CuMoO_4$ ceramic using liquid nitrogen, as shown in figure 3. The polymorph mixture was obtained by cooling

α-CuMoO₄ using liquid nitrogen. 50 ml of liquid nitrogen was added into 2 gm of α-CuMoO$_4$ and kept until entire liquid nitrogen evaporate. The resultant powder appears to be deep brown in color owing to the formation of γ- CuMoO$_4$. The liquid nitrogen helps to attain the γ transition temperature at a fast rate and its volatile nature provides the partial transition of the α to γ, which is
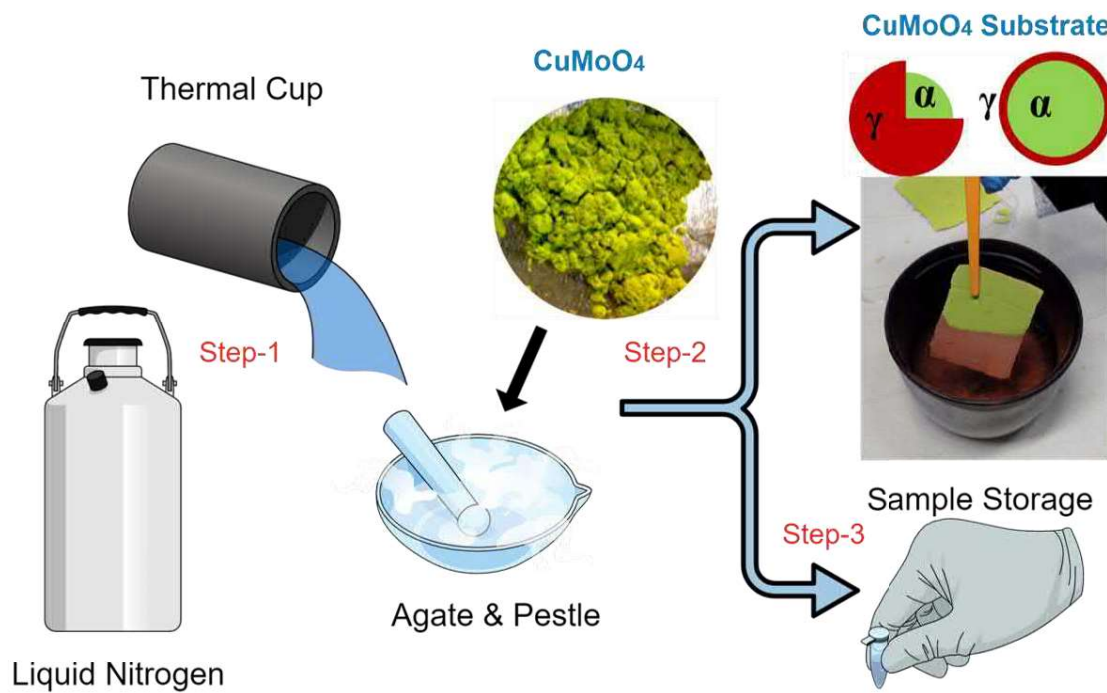
Figure 3. *Preparation of thermochromic CMO polymorph mixture*

mainly confined to the surface atoms, providing a deep brown color to the obtained mixture. This results in the polymorph mixture of α and γ-CMO, with a major phase of α and hence provides the thermochromism in the accessible temperature range of 50-100 °C. The temperature derivatives of the nominal CMO polymorph mixture were obtained by heating it in an oven at different tempeartures of 50,75,100,200 °C ($\pm$ 5 °).

Characterization

Temperature variable X-ray diffraction of the CMO polymorph mixture was examined by X-ray diffractometer (Rigaku Smart Lab 9 kW, Germany) using Co Kα radiation. The microstructure of the obtained CMO polymorph mixture and its temperature derivatives was studied using field emission scanning electron microscopy (Zeiss Ultra Plus, Germany) and high resolution transmission

electron microscopy (JEOL Ltd. Tokyo Japan, JEM-2200FS). The thermal analysis was done using differential scanning calorimetric (DSC) measurement/thermogravimetric analysis (Netzsch 404 F3, Selb). The Raman spectra of the of the nominal CMO polymorph mixture and its temperature derivative compounds were recorded using a spectrometer (LabRam HR800, Horiba Jobin-Yvon, Villeneuve-d'Arcy, France) with signals excited by a 488 nm Ar^+ laser. Fisher Scientific, ESCALAB 250 Xi using the MgKα X-ray source was used for XPS analysis with the spectrometer calibrated with reference energies of Au $4f_{5/2}$ (83.9±0.1 eV) and Cu $2p_{3/2}$ (932.7±0.1 eV). A take-off angle of 90° was maintained between the surface and the analyser for the measurement. For the sample charging correction, the C 1s peak with a binding energy at 284.8 eV corresponding to the surface contamination was used for binding energy calibration.[42] The reflectance spectrum was recorded using a UV-Vis spectrophotometer (Shimadzu UV-2600 spectrophotometer)   with a Shimadzu integrating sphere ISR-2600Plus (covering wavelength range 220-1400 nm).

Results and discussion

The temperature variable X-ray diffraction analysis of the CMO polymorph mixture shown in figure 4, followed by Rietveld refinement using PDXL2 (Analysis incl. Rietveld) (figure S1) indicated that the nominal compound was a mixture of α (JCPDS no: 01-085-1530)[42,43] and γ (JCPDS no:01-0851529) $CuMoO_4$ phases with P1‾ as the space group in the ratio of 65:35% (figure 5(a)). A temperature increase resulted in the γ to α phase transformation as the peaks of the γ phase (2θ = 29.04, 29.2,30.3 °) in the temperature derivative compounds exhibited a decrease in intensity and finally vanished at 200 °C, which is clear from the inset of figure 4. This observation matched well with the obtained percentage of α and γ phase shown in figure 5(a), which shows an increase in % of α phase from 65 to 99.5 and a decrease of the γ phase from 35 to 0.5% over the experimental temperature range. The high intensity peak at 27.6° belonging to α-CMO showed a small shift

towards lower angles and was sharper with temperature, which may correspond to the expansion of the lattice owing to the transformation because α-CMO has a larger cell volume than the γ phase. The crystal structure obtained from the refinement results using VESTA[44] given in figure 5(b) indicated that the α phase consisted of [CuO$_5$] square pyramids and [CuO$_6$] with Mo^{6+} cations at the center of the [MoO$_4$] tetrahedral site, while the γ phase displayed an octahedral coordination of Mo^{6+} and Cu^{2+} ions. A variation in the molybdenum environment from octahedral to tetrahedral and that of
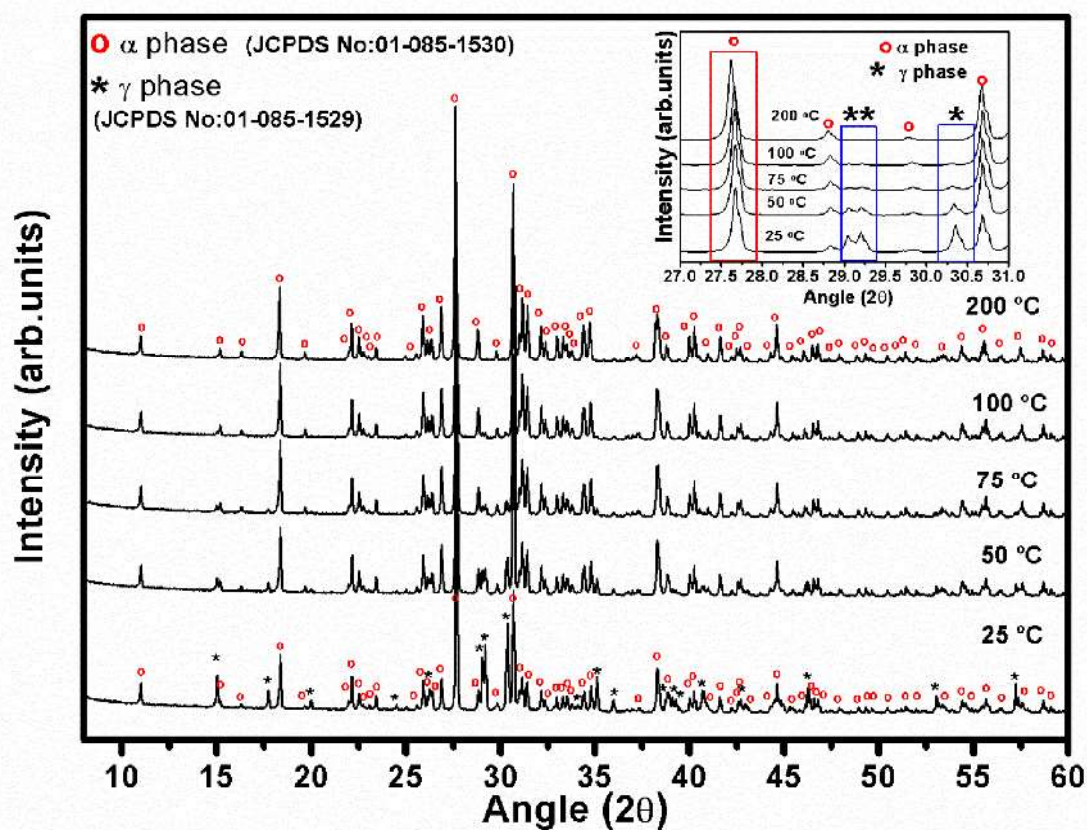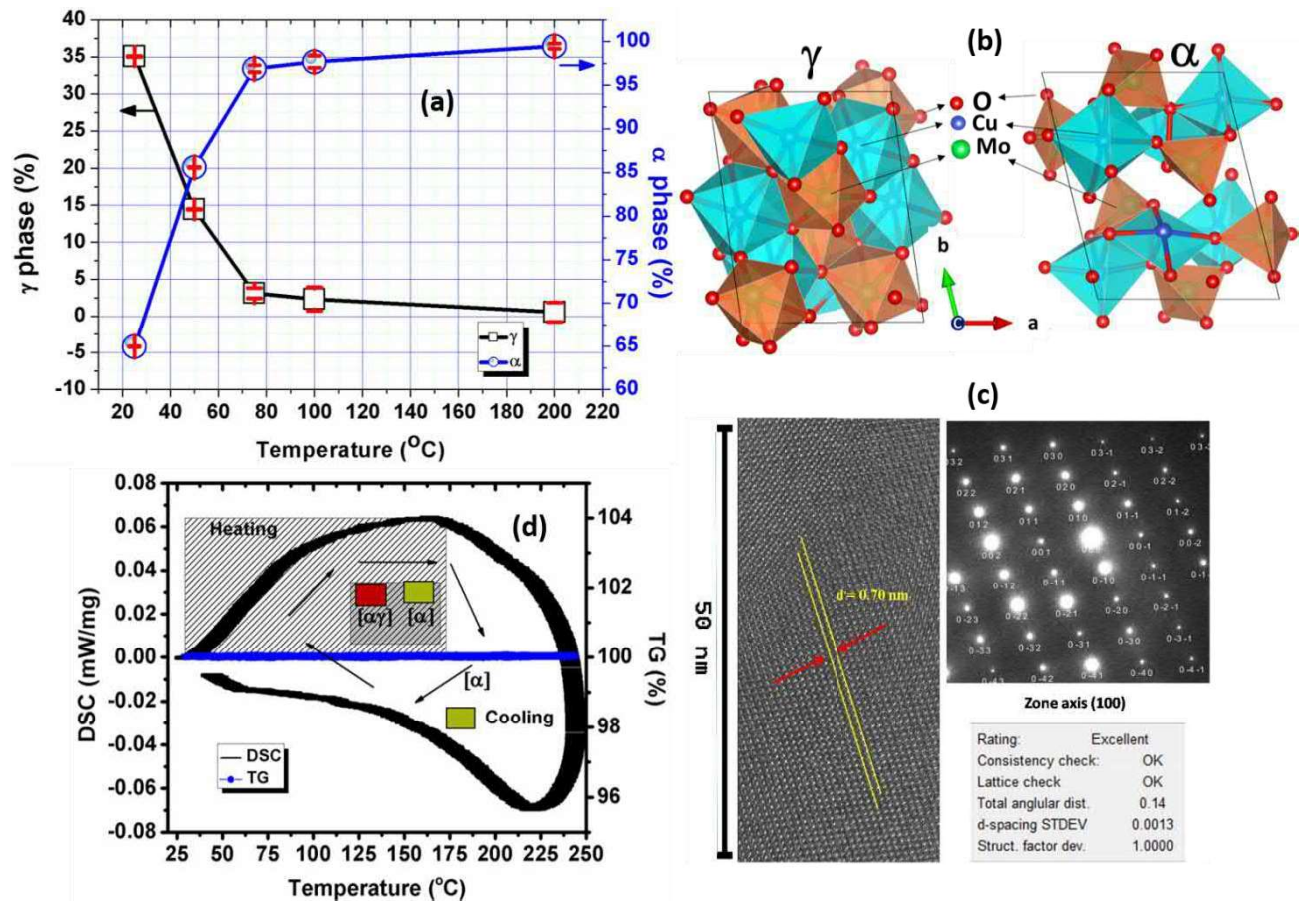

Figure 4. *XRD pattern of nominal CMO polymorph mixture at different temperatures (**Inset figure**: XRD pattern over a 2 θ range of 27-31°)*

1/3 of Cu^{2+} to [CuO$_5$] occurred with the transition from γ to α phase.[15] This possibly corresponds to the cell volume difference of ˷12% between the two phases, with α phase has a = 6.7896 Å, b = 8.3721 Å, c = 9.9057 Å, α = 96.892°, β= 107.008°, χ = 101.128° and V˷519 Å^3 and γ has a = 6.3092, Å, b = 7.9981Å, c = 9.7271Å, α = 103.506°, β = 103.248°, χ = 94.752° and V˷459 Å^3, which is in agreement with the reported results (figure S2).[15,39,40] Figure S2 displays the variation of cell volume as well as lattice parameters with temperature and discrepancy of the data at 200 °C for γ phase may

correspond to its small percentage. Figure 5(c) shows a high resolution TEM image of the dominant α-CMO phase with SAED pattern indexed using CrysTBoxdiffGUI software[45] indicating that the corresponding zone axis was [100]. The images gives an idea on the microstructure of the CMO at the atomic level and the table depicts the accuracy rating of the SAED pattern indexed by the software. The difficulty experienced in thinning down the sample by milling results in the difficulty in obtaining HRTEM images of γ phase that require more specific sample preparation techniques and analysis.

Figure 5. *a) The % variation of α and γ phase in the nominal CMO polymorph mixture with temperature b) crystal structure of α and γ CMO c) α CMO HRTEM, SAED pattern and accuracy table and d) TG-DSC curve of nominal CMO polymorph mixture.*

The TG DSC curve (figure 5(d)) shows a small increase in the energy intake up to the temperature of 150 °C which may correspond to the transition of γ to α phase with no mass loss observed as expected. A maximum energy consumption of only about 0.06 mW/mg observed in the DSC heating curve

highlights the highly sensitive nature and fast response of the nominal CMO polymorph mixture which is advantageous for many practical applications as a prompt permanent temperature recorder. The SEM images of the powdered samples shown in figure S3 give an idea ofthe microstructure of the nominal CMO polymorph mixture and its temperature derivatives. The ceramic had well defined grains owing to the highly crystalline microstructure of the starting material (CMO sintered at 650 °C).
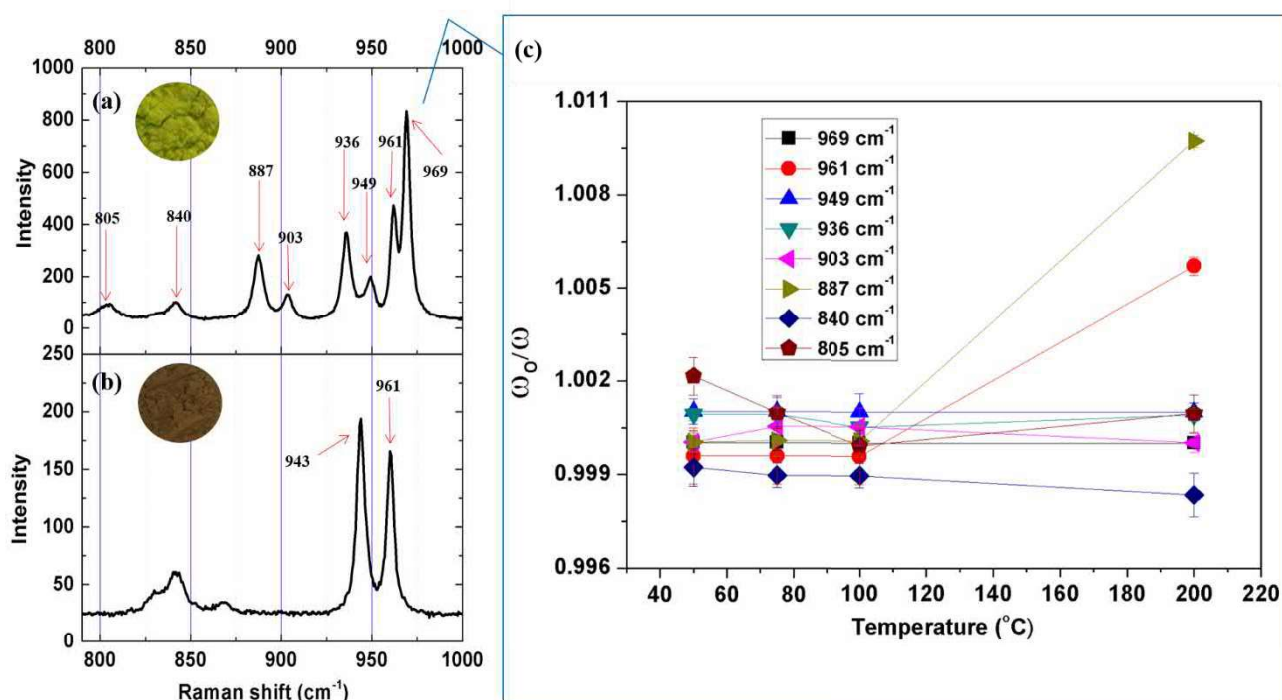

Figure 6. Raman spectra obtained from the a) green region b)red region of nominal CMO polymorph mixture c) Raman shift of each individual mode with respect to temperature (ω_o is the Raman shift of nominal CMO polymorph mixture).

Raman spectra recorded at room temperature for the nominal CMO polymorph mixture and its temperature derivatives showed a decrease in the red region with temperature. The stretching modes of the (O-Mo) could be observed in the high frequency bands in the range 885-1000 cm^{-1} [42,46] and this was investigated to obtain an idea of the change in Mo environment with change intemperature (figure 6). The nominal CMO polymorph mixture gave two spectra, each corresponding to the two colored (red and green) regions in the material. The full spectra of these two regions are given as figure S4 in the supporting information. The spectra corresponding to the green region (figure 6a)) showed peaks

corresponding to the MoO_4 tetrahedral form in agreement with the reported results.[42] However, the spectrum observed in the red region (figure 6(b)) exhibited a peak around 943 and 961 cm^{-1}, which may correspond to the Mo octahedral and tetrahedral forms, indicating the presence of mixed phase [42,47] even though the color appeared red. This may attribute to the transformation of the surface atoms to the γ phase due to the quenching. Similarly to the nominal CMO polymorph mixture, the spectra corresponding to the red and green regions were obtained for the temperature derivative at 50 °C, while only green region spectra were obtained for temperatures 75 °C and above. This point to the transformation of γ to α with temperature in agreement with the XRD results and hence resulting in the change in optical properties. Since the spectra of the green region figure 6(a) was observed in all the measured samples, figure 6(c) depicts the variation of Raman shift of the nominal CMO polymorph mixture with its temperature derivatives for each peak (ω_o/ω) with temperature. The temperature did not exhibit much shift on these bonds with a small red shift observed for the bonds (887 and 961 cm^{-1}) that may relate to the γ to α transformation.

A detailed study of the oxidation of the nominal CMO polymorph mixture and its temperature derivatives was characterized by X-ray photoelectron spectroscopy (XPS) and the spectra of Cu 2p, Mo 3d are shown in figure 7 (a and b) respectively. The high-resolution Cu 2p spectrum given in figure 7(a) showed a spin orbital splitting components of $2P_{3/2}$ and $2p_{1/2}$ by about 19.6-19.8 eV with binding energies of 934.5-935.04 eV ($2P_{3/2}$) and 953.8-954.6 eV ($2P_{1/2}$) with temperature. The Cu^{2+} strong satellite peaks further confirmed the 2^+ oxidation state of Cu in these measured compounds.[42,48,49] A spin orbital splitting of about 3.13- 3.15 eV observed for $3d_{5/2}$ and $3d_{3/2}$ indicated the 6^+ oxidation state of Mo in the measured samples as presented by the high resolution Mo 3d spectra (figure 7(b)).[42,50] The binding energy was in the range of 232.3 - 232.5 eV for Mo $3d_{5/2}$ and 235-235.8 eV as observed from the Mo 3d spectra of the nominal compound and its temperature derivatives. A small increase in the binding energies of Cu2p and Mo3d spectra was observed and may relate to the corresponding change in their environment from octahedral to square pyramid and

tetrahedral respectively.[51] The fitted binding energies of Cu2p and Mo3d are given in supporting information Table S2. The results revealed that the Cu2p and Mo3d spectra obtained for the nominal CMO mixture were similar to earlier reports[42] which confirms the oxidation state of Cu and Mo in the mixture.
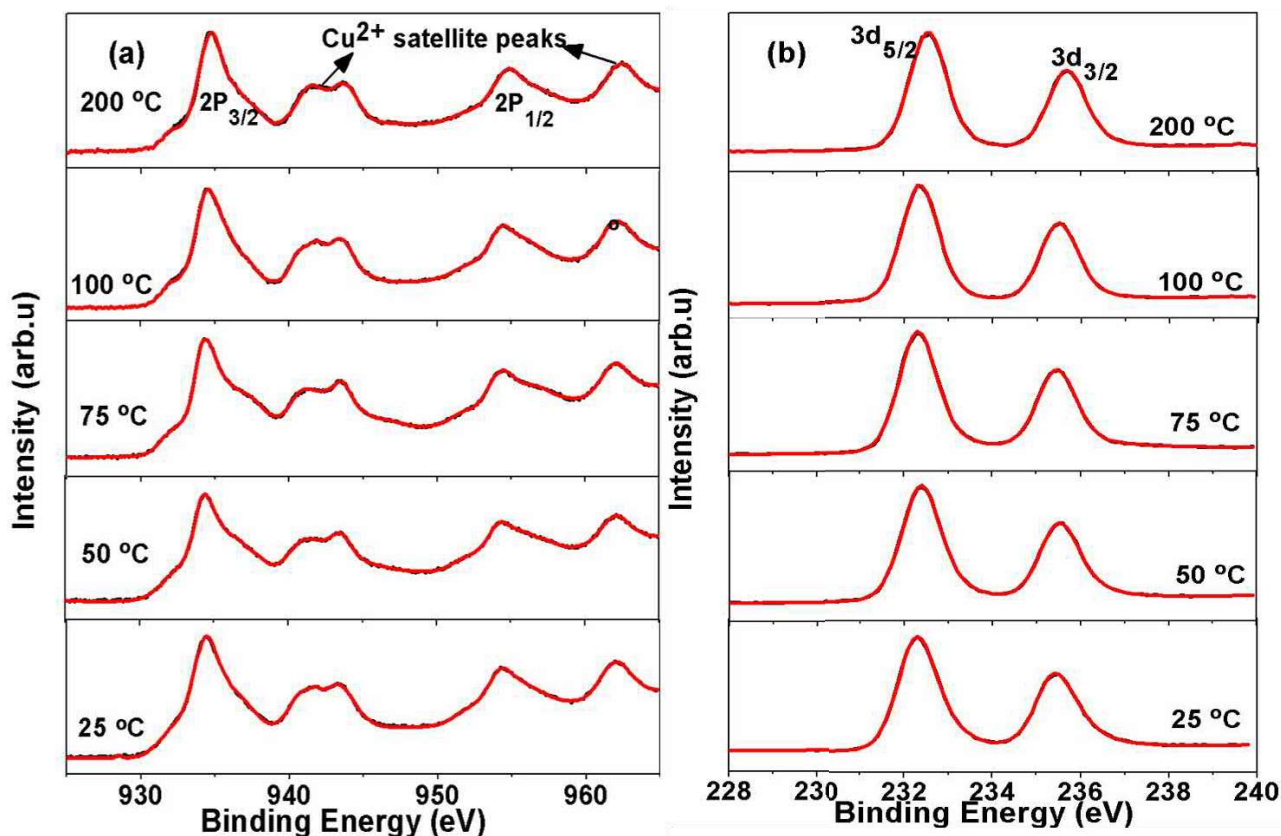
Figure 7. *a) High resolution of Cu2p spectra for nominal CMO polymorph mixture and its temperature derivatives and b) High resolution of Mo3d spectra for nominal CMO polymorph mixture and its temperature derivatives.*

Reflectivity spectra of the nominal CMO polymorph mixture and its different temperature derivatives recorded at room temperature showed an evolution around 615-570 nm from the red to the green region as shown in figure 8(a and b),which explained its thermochromic behavior and confirmed, the change in the composition and structure of the polymorph mixture with temperature. The nominal mixture with maximum reflectance at around 613 nm had a deep brownish color which changed to light brown (~605 nm) to yellowish green (~600 nm) to light green (~590 nm) to bright green color (~570 nm) respectively at 50, 75, 100 and 200 °C.
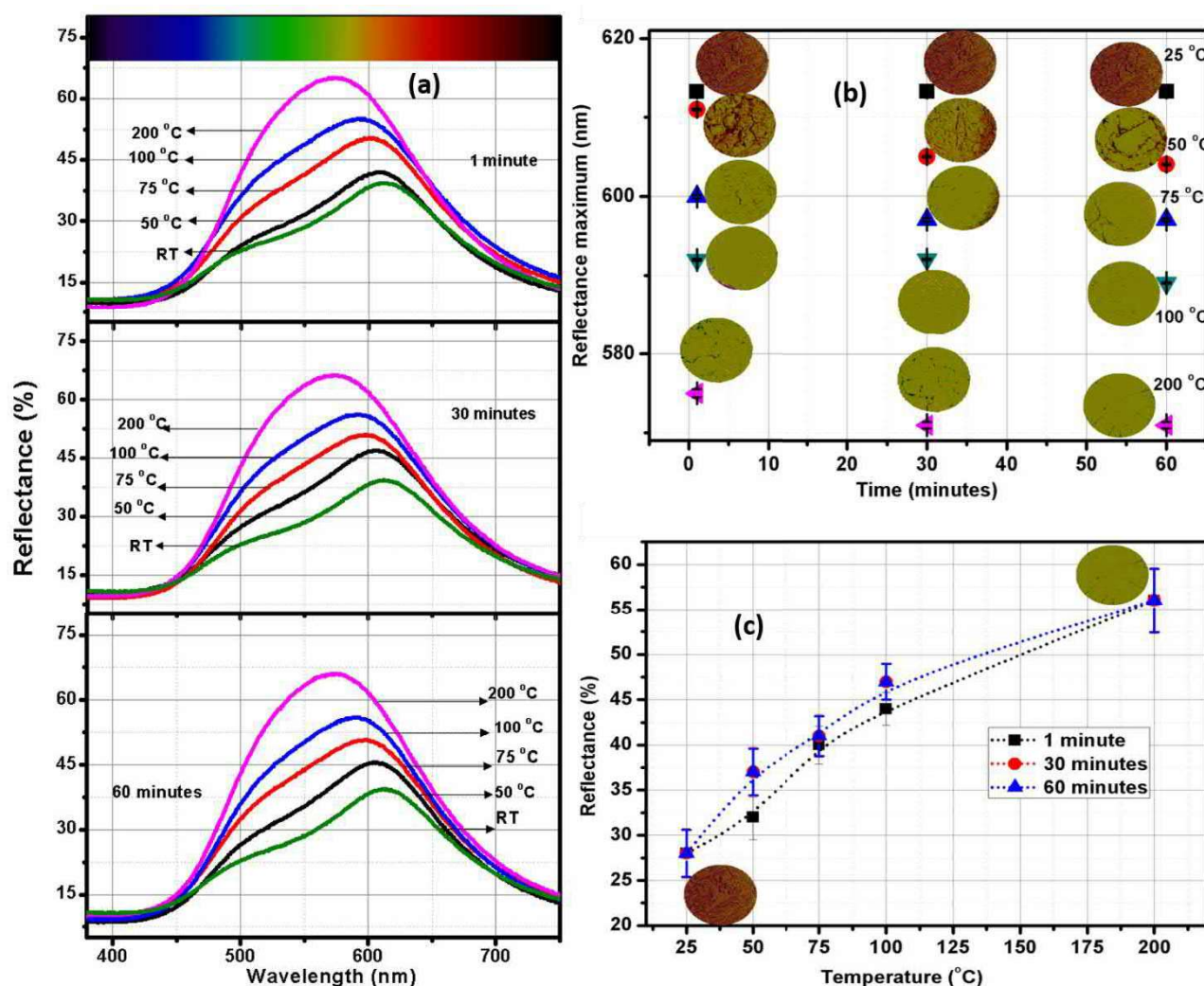
Figure 8. *a) Reflectance spectra b) Reflectance maximum of the nominal CMO polymorph mixture and its temperature derivatives at different time durations c) The reflectivity (%) change from deep brown to green region in the measured temperature range of 25-200 °C.*

The color of the α phase is reported to be due to the charge transfer $O^{2-} \rightarrow Cu^{2+}$ transitions and crystal field Cu^{2+} d-d transitions owing to the CuO_5 and CuO_6 polyhedral, while that of crystal field transitions due to the CuO_6 octahedral contributes color in γ phase.[39,40] The duration of temperature exposure had only a minor effect as evident from figure 8(b), particularly at temperature above 50 °C. The reflectance spectra at 50 °C changed around 611-604 nm with 1, 30 and 60 minutes exposure of the nominal compound making it a useful temperature-time scale indicator at low temperature. However, when exposed to temperatures of 75 °C and above, it exhibited a fast response of less than 1 minute, indicating its application as a high speed temperature indicator as confirmed from the

thermal analysis. The percentage of reflectance also increased with increase in temperature as the reflectivity also depends on the ratio of the α/γ change with temperature.[19] The evolution of the reflectivity from the deep brown to the green region in the measured temperature range of 25-200 °C, over a duration of 60 minutes is displayed in figure 8(c). The temperature exposure duration had little effect on the reflectivity, as expected. During heating, the $\gamma \rightarrow \alpha$ transition changed the ratio of the phases as the dark colored nominal compound changed to the bright colored temperature derivative, making the CMO polymorph mixture a promising material for interacting with thereal world in a more immediate way, similar to the natural andbiological logic.

Conclusion

An irreversible thermochromic $CuMoO_4$ polymorph mixture was prepared by asimple cryogenic quenching process (liquid nitrogen) of α-$CuMoO_4$ prepared by the solid state ceramic route. The process resulteda polymorph mixture with a non-uniform combination of α and γ phase of $CuMoO_4$ (α:γ = 65:35) as confirmed by the insitu XRD analysis and refinement, with the γ phase mainly confined to the outer surface of α phase, which was responsible for its deep brown color. The transformation of the γ phase to theα phase with temperature resulted in the thermochromic behavior, exhibiting a color change to light brown, yellowish green , light green and bright green respectively at 50, 75, 100 and 200 °C as observed from the reflectance spectra. Moreover, the time duration had little effect on the chromism exhibited by this material indicating it's fast response behavior, as observed from the thermal analysis. The Raman spectrum analysis also revealed the presence of both phases at lower temperature. The absence of any change in the chemical composition by this cryogenic quenching was confirmed by XPS analysis. Hence, this unique $CuMoO_4$ polymorph mixture can open up new opportunities in the technology as a simple, smart, permanent and fast material temperature recorder.

Acknowledgment

Supporting information

Comparison of the present work with the reported inorganic thermochromic materials; XRD and the refinement parameters of the nominal CMO polymorph mixture and its temperature derivatives; Cell volume, lattice parameters of α and γ-CMO phase obtained from temperature variable XRD measurements; SEM images of the nominal CMO polymorph mixture and its temperature derivatives; Raman spectra obtained from the green region and red region of nominal CMO polymorph mixture over 100-1000 cm^{-1}; Fitted binding energies in ev of Cu2p and Mo3d of nominal CMO polymorph mixture and its temperature derivatives.

Reference

1. Schwart, M.; Lenzini, G.; Geng, Y.; Rønne, P. B.;Ryan, P. Y. A.; Lagerwall, J. P. F.Cholesteric Liquid Crystal Shells as Enabling Material for Information-Rich Design and Architecture.*Adv. Mater.***2018**, *30*, 1707382 (1-19).

2. Zhang, X.; Chen, L.; Lim, K. H.; Gonuguntla, S.; Lim, K. W.; Pranantyo, D.; Yong, W. P.; Yam, W. J. T.; Low, Z.; Teo, W. J.; Nien, H. P.; Loh, Q. W.; Soh, S. The Pathway to Intelligence: Using Stimuli-Responsive Materials as Building Blocks for Constructing Smart and Functional Systems. *Adv. Mater.***2019**, *31*, 1804540 (1-48).

3. Science Direct, Smart Materials, https://www.sciencedirect.com/topics/chemistry/smart-material, accessed: June, 2019

4. Levi, D. S.; Kusnezov, N.; Carman, G. P. Smart Materials Applications For Pediatric Cardiovascular Devices. *Pediatr. Res.***2008**, *63*, 552.

5. Roy, I.; Gupta, M. N.Smart Polymeric Materials: Emerging Biochemical Applications, Review. *Chem. Biol.***2003**, *10*, 1161.

6. Coyle, S.; Wu, Y.; Lau, K.; De Rossi, D.; Wallace, G.; Diamond,D. Smart Nanotextiles: A Review of Materials and Applications. *MRS Bulletin***2007**, *32*, 434.

7. UK.Essays, Applications and Types of Smart Materials Engineering Essay, https://www.ukessays.com/essays/engineering/applications-and-types-of-smart-materials-engineering-essay.php?vref=1, accessed: June 2019.

8. Strock, H. Smart Materials Systems: Emerging Automotive Applications, *Mater. Technol.***1995**, *10*,159.

9. Manz, H.; Schmidt, K. On the Application of Smart Materials in Automotive Structures, Vol. 13 (Eds: K. Grassie, E. Teuckhoff, G. Wegner, J. Hausselt, H. Hanselka), Wiley-VCH Verlag GmbH, Weinhein **2000**.

10. Worldatlas, 10 Animals that can change colors, https://www.worldatlas.com/articles/10-animals-that-can-change-colors.html, accessed: June 2019.

11. Ferrara, M.; Bengisu, M. Materials that Change Color Smart Materials, Intelligent Design, Springer, New York **2014**.

12. Nassau, K. The Physics and Chemistry of Color, John Wiley and Sons Inc., New York **1983**.

13. Eom, S. H.; Kim, D. J.; Yu, Y.-M.; Choi, Y. D. Temperature-Dependent Absorption Edge in $AgGaS_2$ Compound Semiconductor. *J. Alloys Compd.***2005**, *388*, 190.

14. Nunes, G. G.; Friedermann, G. R.; dos Santos,J. L. B.; Herbst, M. H.; Vugman, N. V.; Hitchcock, P. B.; Leigh,G. J.; Sa´, E. L.; da Cunha, C. J.; Soares, J. F. The First Thermochromic Vanadium (IV) Alkoxide System. *Inorg. Chem. Commun.***2005**, *8*, 83.

15. Gaudon, M.; Deniard, P.; Demourgues, A.; Thiry, A. –E.; Carbonera, C.; Le Nestour, A.; Largeteau, A.; Létard, J.-F.; Jobic, S. Unprecedented "One-Finger-Push"-Induced Phase Transition With a Drastic Color Change in an Inorganic Material. *Adv. Mater.***2007**, *19*, 3517.

16. Science Direct, Thermochromic Material, https://www.sciencedirect.com/topics/engineering/thermochromic-material, accessed: June, 2019.

17. Wang, S.; Liu, M.; Kong, L.; Long, Y.; Jiang, X.; Yu, A. Recent Progress in VO_2 smart Coatings: Strategies to Improve The Thermochromic Properties. *Prog. Mater. Sci*. **2016**, *81*, 1.

18. Ehrenberg, H.; Weitzel, H.; Paulus, H.; Wiesmann, M.; Wltschek, G.; Geselle, M.; Fuess, H. Crystal Structure And Magnetic Properties of $CuMoO_4$ At Low Temperature (γ-Phase). *J. Phys. Chem. Solids***1997**, *58*, 153.

19. Thiry, A. –E.; Gaudon, M.; Payen, C.; Daro, N.; Létard, J.-F.;Gorsse, S.;Deniard, P.; Rocquefelte, X.; Demourgues, A.; Whangbo, M.-H.; Jobic, S. On the Cyclability of the Thermochromism in $CuMoO_4$ and Its Tungsten Derivatives$CuMo_{1-x}W_xO_4$ (x < 0.12). *Chem. Mater.***2008**, *20*, 2075.

20. Nguyen, D. K.; Bach, Q.-V.; Lee, J.-H.; Kim, I.-T. Synthesis and Irreversible Thermochromic Sensor Applications of Manganese Violet, *Materials* **2018**, *11*, 1693.

21. Day, J. H. Thermochromism of Inorganic Compounds. *Chem. Rev.***1968**, 68, 649.

22. Warwick, M. E. A.;Binions. R. Advances in Thermochromic Vanadium Dioxide Films. *J. Mater. Chem. A***2014**, *2*, 3275.

23. Gaudon, M.; Carbonera, C.; Thiry, A. -E.; Demourgues, A.; Deniard, P.; Payen, C.; Le´tard, J.-F.; Jobic, S. Adaptable Thermochromism in the $CuMo_{1-x}W_xO_4$ Series (0 < x < 0.1): A Behavior Related to a First-Order Phase Transition with a Transition Temperature Depending on x. *Inorg. Chem.* **2007**, *46,* 10200.

24. Sun, W.; Li, Y.; Shi, W.; Zhao, X.; Fang, P. Formation of AgI/TiO_2Nanocomposite Leads to Excellent Thermochromic Reversibility and Photostability. *J. Mater. Chem.***2011**, *21*, 9263.

25. Kumar, S.; Qadir, A.; Maury, F.; Bahlawane, N. Visible Thermochromism in Vanadium Pentoxide Coatings. *ACS Appl. Mater. Interfaces* **2017**, 9, 21447.

26. Liu, H.; Qi, H.; Yuan, L.; Wang, B.; Hou, C.; Feng, S. Design Principles for 3d Electron Transfer in a Ga-Based Garnet To Enable High-Performance Reversible Thermochromic Material Color Maps. *Chem. Mater.* **2019**, *31*, 1048.

27. Nguyen,D. K.; Bach, Q.-V.; Kim, B.; Lee, H.; Kang, C.; Kim, I.-T. Synthesis of Cr-doped Al_2O_3 by PechiniSol-Gel Method and its Application for Reversible Thermochromic Sensors. *Mater. Chem. Phys.* **2019**, *223*, 708.

28. Salek, G.; Devoti, A.; Lataste, E.; Demourgues, A.; Garcia, A.; Jubera, V.; Gaudon, M. Optical Properties Versus Temperature of Cr-doped γ- and α-Al_2O_3:Irreversible Thermal Sensors Application. *J. Lumin.* **2016**, *179*, 189.

29. Zhu, Y.; Xu, G.; Guo, T.; Hou, H.; Tan, S. Preparation, Infrared Emissivity And Thermochromic Properties of Co doped ZnO by Solid State Reaction. *J. Alloy. Compd.* **2017**, *720*, 105.

30. Buxbaum, G.; PfaffI, G. Industrial Inorganic Pigments, Wiley-VCH Verlag GmbH & Co. KGaA, Weinheim, **2005**.

31. Shapovalov, V. I.; Lapshin, A. E.; Komlev, A. E.; Komlev, A. A. Crystallization and Thermochromism in Tungsten Oxide Films Annealed in Vacuum. *Tech.* Phys. Lett.**2012**, *38*, 555.

32. Lataste, E.; Demourgues, A.; Salmi, J.; Naporea, C.; Gaudon, *Dyes.* M.Thermochromic Behaviour (400 < T ˚C < 1200 ˚C) of Barium Carbonate/Binary Metal Oxide Mixtures. *DyesPigm.***2011**, *91*, 396.

33. Lucht, B. L.; Euler W. B. (Rhode Island Board of Governors for Higher Education), US, WO/2009/137709.

34. Kwan, W. S. V. (Sanford LP), US, US8664156B2.

35. Lempereur, C.; Andral, R.; Prudhomme, J. Y. Surface Temperature Measurement on Engine Components by Means of Irreversible Thermal Coatings. *Meas. Sci. Technol.* **2008**, *19*, 105501.

36. Pelvich, C.W.;.Foulk, D. L.; Polec, T. W. (Honeywell International Inc), EP1959246 A2.

37. Hayakawa, T.; Maruyama, H.; Watanabe, T.; Arai, F.Three-Dimensional Blood Vessel Model with Temperature-Indicating Function for Evaluation of Thermal Damage during Surgery. *Sensors***2018**, *18*, 345.

38. Wiesmann, M.; Ehrenberg, H.; Miehe,G.; Peun, T.; Weitzel,H.; Fuess, H. p-T Phase Diagram of $CuMoO_4$. *J. Solid State Chem.***1997**, *132*, 88

39. Hernández, D.; Rodríguez, F.; Garcia-Jaca, J.; Ehrenberg, H.; Weitzel, H. Pressure-Dependence on The Absorption Spectrum Of $CuMoO_4$: Study of the Green $\rightarrow$ brownish-Red Piezochromic Phase Transition At 2.5 Kbar. *Phys. B***1999**, *265*, 181.

40. Rodríguez, F.; Hernández, D.; Garcia-Jaca, J.; Ehrenberg, H.; Weitzel, H. Optical Study of Piezochromic Transition in $CuMoO_4$ by Pressure Spectroscopy.*Phys. Rev. B***2000**, *61*, 16497.

41. Steiner,G.; Salzer,R.; Reichelt, W. Temperature Dependence of the Optical Properties of $CuMoO_4$. *FreseniusJ. Anal. Chem.***2001**, *370*, 731.

42. Joseph, N.; Varghese, J.; Siponkoski, T.; Teirikangas, M.; Sebastian, M. T.; Jantunen, H. Glass Free $CuMoO_4$ Ceramic with Excellent Dielectric Properties for Ultra-Low Temperature Cofired Ceramic Applications. *ACS Sustain. Chem. Eng.* **2016**; 4, 5632.

43. Joseph, N.; Varghese, J.; Teirikangas, M.; Jantunen, H. Ultra-Low Sintering Temperature Ceramic Composites of $CuMoO_4$ through Ag_2O Addition for Microwave Applications.*Composites Part B* **2018**,*141*, 214.

44. Momma, K.; Izumi, F. VESTA 3For Three-Dimensional Visualization Of Crystal, Volumetric and Morphology Data. *J. Appl. Cryst.***2011**, *44*, 1272.

45. Klinger, M. More Features, More Tools, More CrysTBox. *J. Appl. Cryst.***2017**, *50*, 1226.

46. NIST, XPS Database, http://srdata.nist.gov/xps/main_search_menu.aspx, accessed: June, 2019.

47. Beisinger,M. C.; Lau,L. W. M.; Gerson, A. R.; Smart, R. S. C.Resolving Surface Chemical States in XPS Analysis of First Row Transition Metals Oxides and Hydroxides:Sc, Ti, V, Cu and Zn. *Appl. Surf. Sci.***2010**, *257*, 887.

48. Brezesinski, T.; Wang, J.; Tolbert, S. H.; Dunn, B. Ordered Mesoporous α-MoO$_3$ with Iso-oriented Nanocrystalline Walls for Thin-Film Pseudo Capacitors. *Nat. Mater.***2010**, *9*, 146.

49. Reddy, B. M. B.; Chowdhury, B.; Reddy, E. P.; Fernández, A. *Appl. Catal., A***2001**, *213*, 279.

50. Nazrl, G.-A.; Julien, C.Far-Infrared and Raman Studies of Orthorhombic MoO$_3$ Single Crystal. *Solid State Ionics***1992**, *53-56*, 376.

51. Hardcastle, F. D.; Wachs, I. E. Determination of Molybdenum-Oxygen Bond Distances and Bond Orders by Raman Spectroscopy *J. Raman Spectrosc.* **1990**, *21*, 683.

Graphical Abstract
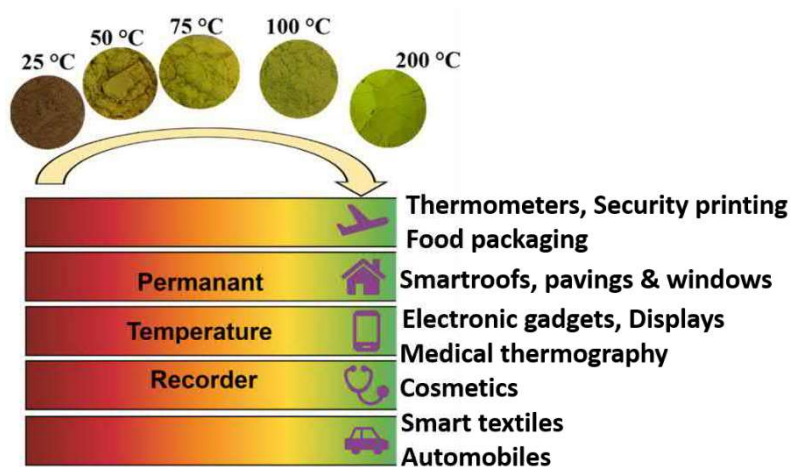
Temperature Responsive Copper Molybdate Polymorph Mixture

Supporting information

A Temperature Responsive Copper Molybdate Polymorph Mixture Near to Water Boiling Point by a Simple Cryogenic Quenching Route

Nina Joseph*, Jobin Varghese, Merja Teirikangas, and Heli Jantunen

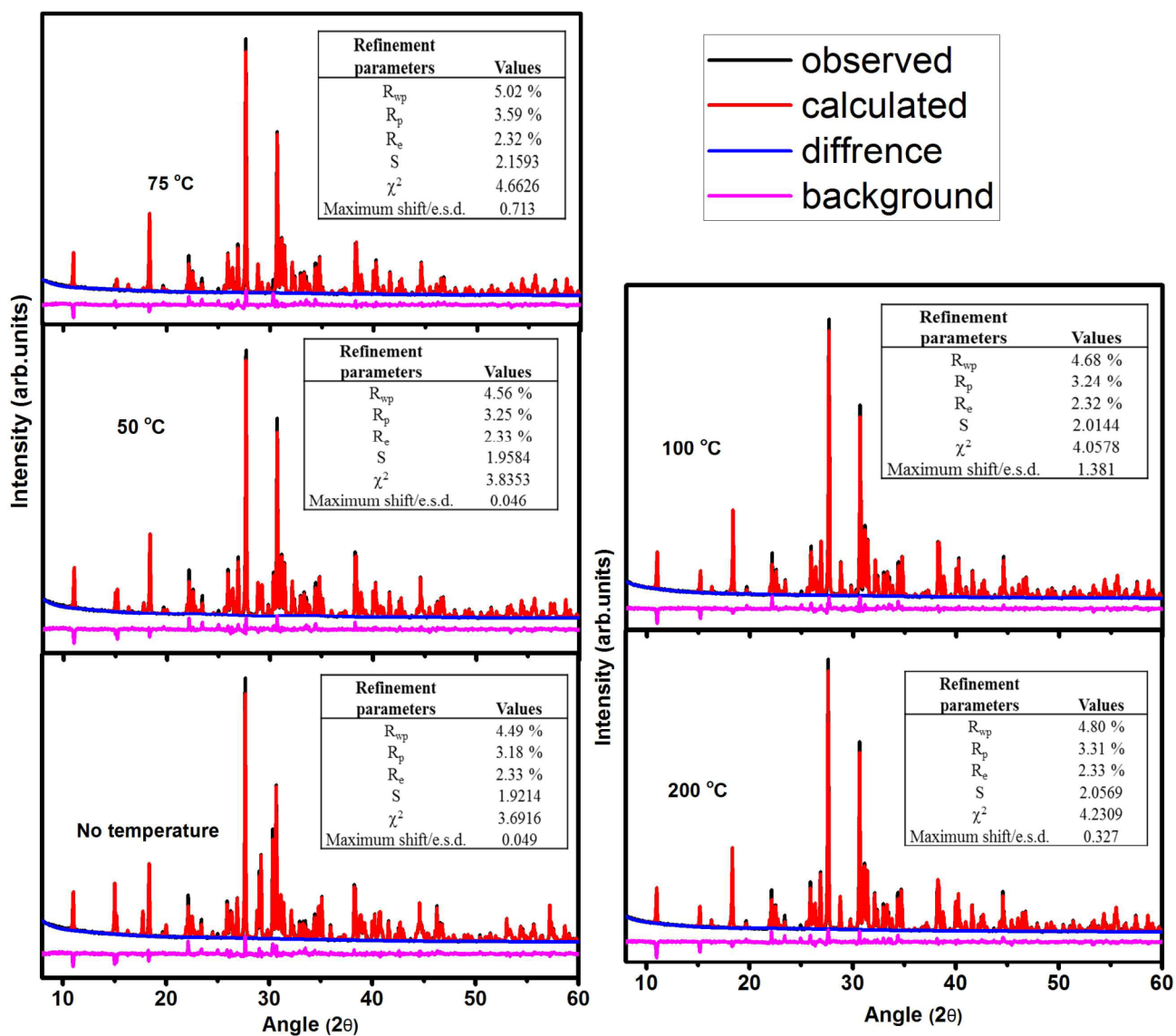Microelectronics Research Unit, Faculty of Information Technology and Electrical Engineering,

University of Oulu, Finland, P.O. Box 4500, FI-90014.

*Corresponding author: Nina Joseph

Email: ninajoseph11@gmail.com

Table S1: Comparison of the present work with the reported inorganic thermochromic materials

| Materials	Temperature range (°C)	Color change
Reversible thermochromic mterials		
$CuMoO_4$ [18,19]	-73	green $\leftrightarrow$ reddish brown
$[NH_2(C_2H_5)_2]2CuCl_4$ [20]	38	deep green$\leftrightarrow$yellow
Ag_2HgI_4 [21]	50	yellow$\leftrightarrow$ orange
VO_2 [22]	68	-
Cu_2HgI_4 [21]	25-85	red $\leftrightarrow$black-brown
$CuMo_{0.9}W_{0.1}O_4$ [19, 15, 23]	85	light green $\leftrightarrow$ reddish brown
HgI_2 [20]	127	red$\leftrightarrow$yellow
AgI [21]	147	yellow$\rightarrow$redbrown
$AgI-TiO_2$ [24]	150	
V_2O_5 [25]	25-300	bright yellow$\leftrightarrow$deep orange
	100,200,300	
$Cr^{3+}/Mn^{3+}/Fe^{3+}/Co^{3+}$-doped $Er^3Ga_5O_{12}$ [26]	460	green $\leftrightarrow$ yellow green red color$\leftrightarrow$dark red yellow-green$\leftrightarrow$yellow light cyan $\leftrightarrow$ yellow
Cr doped Al_2O_3 [27, 28]	25-600 250,400-450,	red/pink$\leftrightarrow$green/grey
ZnO [29, 30]	>500	white $\leftrightarrow$ yellow
WO_3 [30, 31]	>500	light $\leftrightarrow$deep blue
Co^{2+}doped ZnO [29]	>700	green becomes darker
Irreversible thermochromic mterials		
$CuMoO_4$ polymorph mixture [Present work]	50, 75, 100 200	deep brown $\rightarrow$ light brown deep brown $\rightarrow$ yellow green deep brown $\rightarrow$light green deep brown $\rightarrow$ bright green
CuI [20]	60-62	
NH_4VO_3 [20]	150 170	white$\rightarrow$brown brown$\rightarrow$black
$CoCO_2$ [20]	330	violet$\rightarrow$black
$MnNH_4P_2O_7$ [20]	400	violet$\rightarrow$white
NiC_2O_4 [20]	410	lightblue$\rightarrow$black
$BaCO_3-WO_3$ [32]	500-1000	pastel green $\rightarrow$ cream
$BaCO_3-Bi_2O_3$	500	
$BaCO_3-V_2O_5$	500	
$BaCO_3-Y_2Ti_2O_7$	700	
$BaCO_3-ZnO:Co$	700	
$BaCO_3-CoAl_2O_4$	800-900	dark blue $\rightarrow$ dark grey
$BaCO_3-Cr_2O_3$	800	
$BaCO_3-Fe_2O_3$	800	
$BaCO_3-NiO$	900	

Figure S1: *XRD and the refinement parameters of the nominal CMO polymorph mixture and its temperature derivatives*
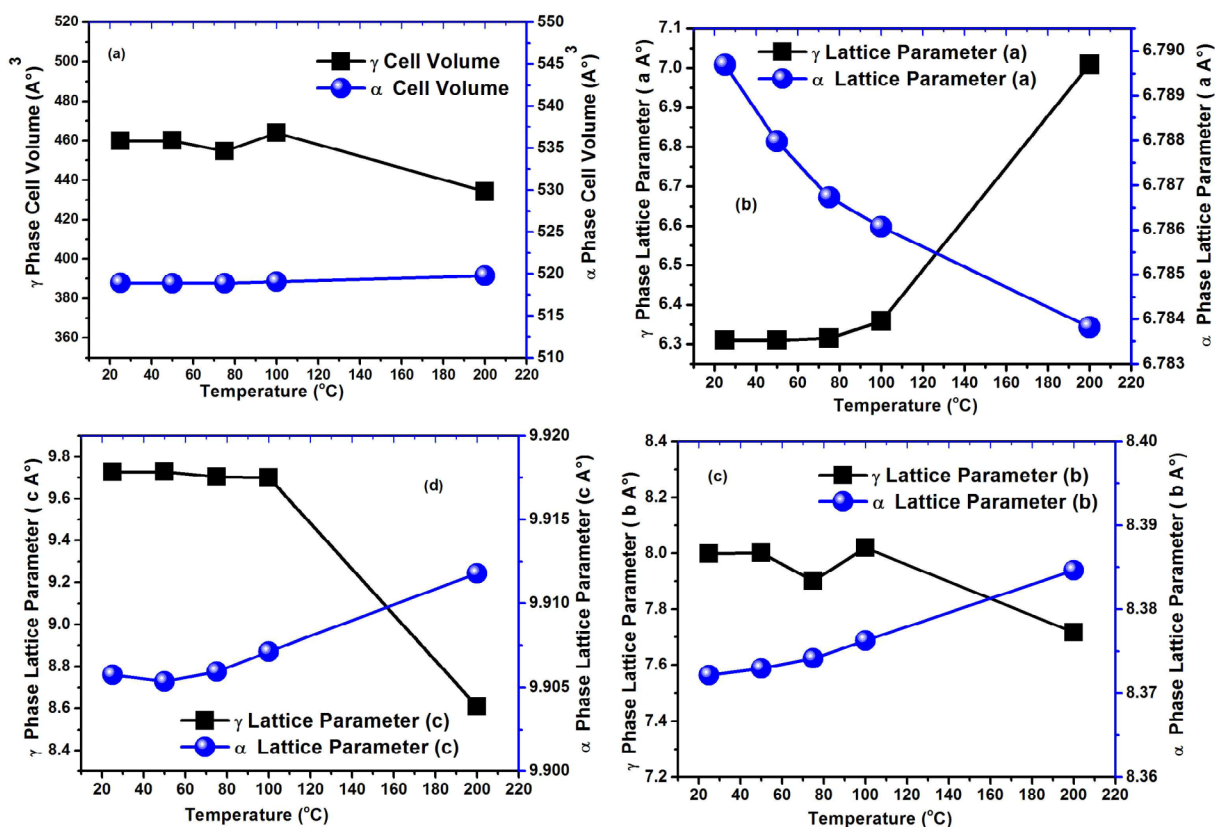
Figure S2*: (a) Cell volume, lattice parameter (b) a (c) b and (d) c of α and γ CMO phase obtained from temperature variable XRD measurements.*
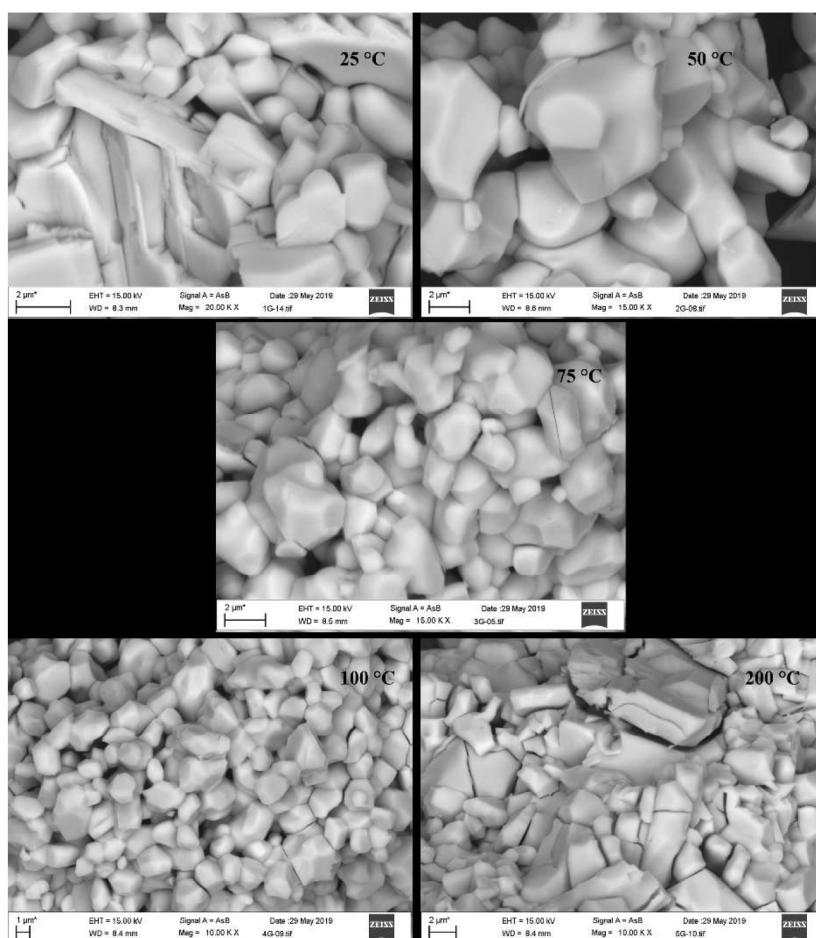
Figure S3: *SEM images of the nominal CMO polymorph mixture and its temperature derivatives.*
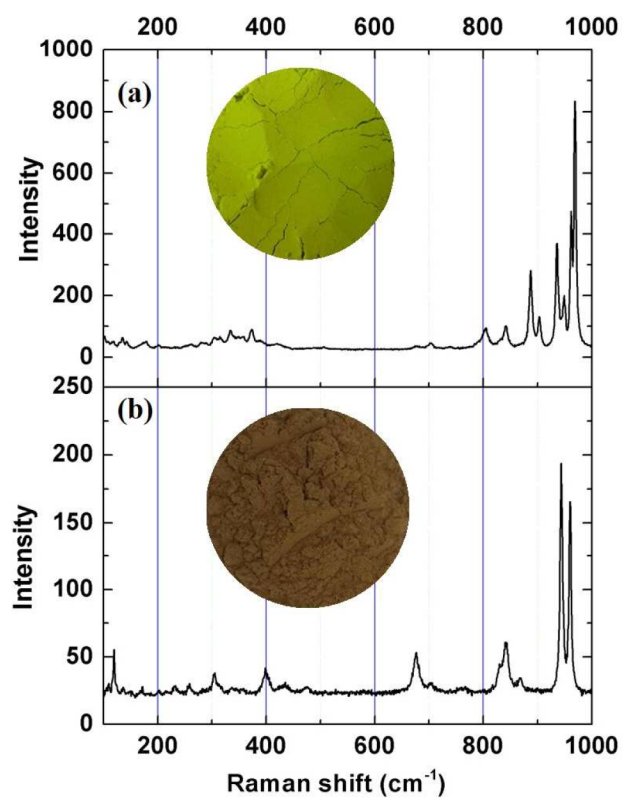
Table S2: *Fitted binding energies in ev of Cu2p and Mo3d of nominal CMO polymorph mixture and its temperature derivatives.*

Sample	Cu		Mo	
	Cu $2p_{3/2}$	Cu $2p_{1/2}$	Mo $3d_{5/2}$	Mo $3d_{3/2}$
Nominal CMO polymorph mixture	934.54	954.3	232.35	235.49
@ 50 ℃	934.5	954.29	232.41	235.55
@75 ℃	934.33	953.88	232.34	235.47
@ 100 ℃	934.90	954.50	232.36	235.51
@200 ℃	935.04	954.68	232.55	235.70